

Overview

Emplacement of infrastructure, such as renewable energy converter foundations, cables, or pipelines, on or below the seabed requires knowledge of the engineering properties of the marine soils that could potentially support them (Eamer et al., 2022). Generally, there is a need to expand the geotechnical characterisation of seabed sediments over wide regions of Pacific Canada's inner shelves (an example of another record includes Ouellette et al., ND). In late 2021, the scientific expedition 202106PGC aboard the CCGS Vector resulted in a number of gravity cores from which whole round samples could be extracted for advanced geotechnical testing (Figure 1). Coring targets were exposures of glaciomarine sediments – overlying Holocene muds are unlikely to have ideal geotechnical properties for infrastructure emplacement, and sandy sediments and/or glacial diamicton are challenging to sample with a shallow penetrating gravity corer. Advanced geotechnical tests were conducted at the Geological Survey of Canada-Atlantic's (GSC-A) Geotechnical Laboratory to develop a geotechnical characterisation of glaciomarine sediments that can be used to evaluate seabed foundation conditions. (see Eamer et al., 2022 for a discussion on the geotechnical data required to evaluate OWT seabed foundation conditions and the GSC-A geotechnical laboratory testing capabilities).

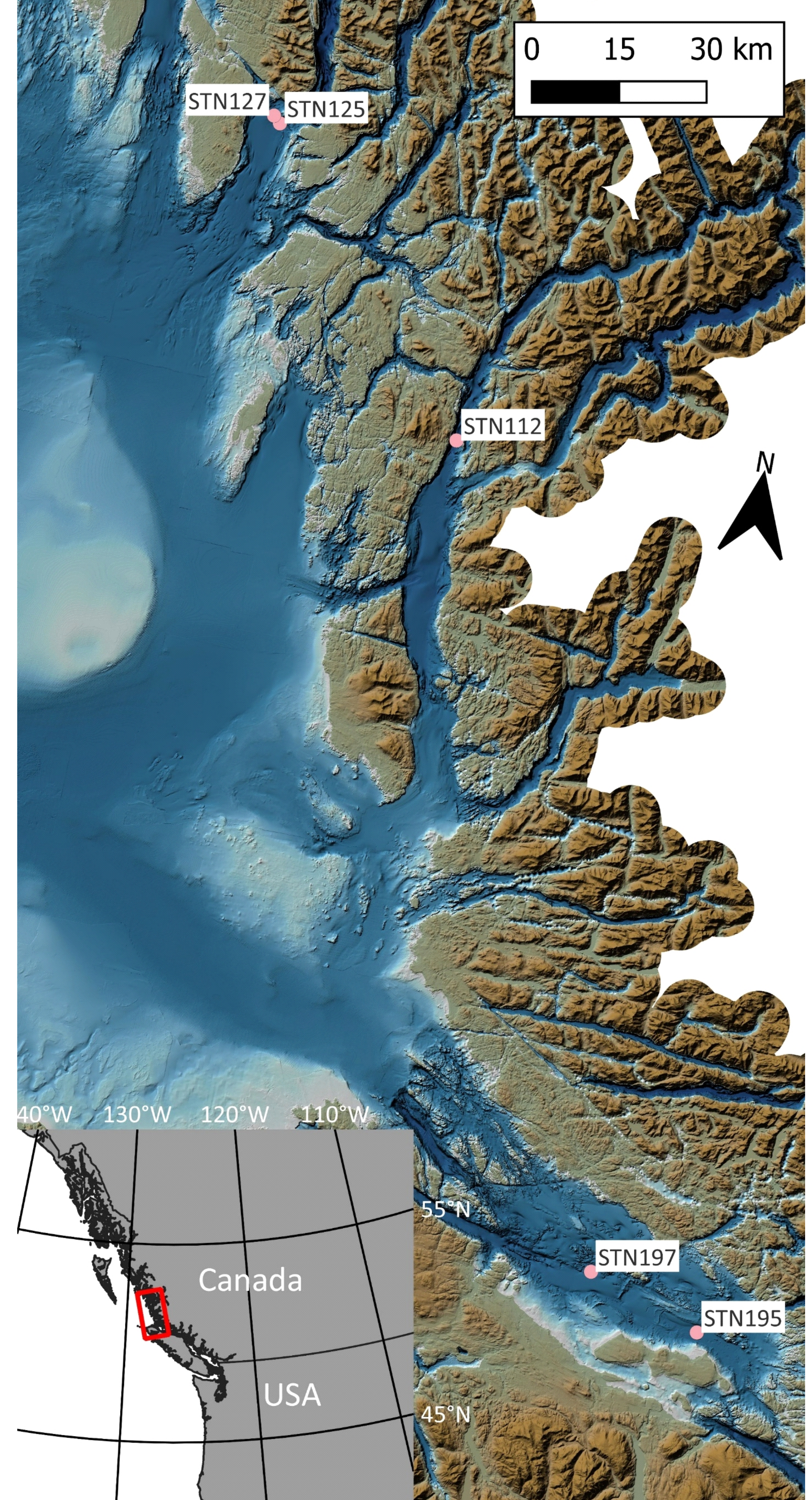


Figure 1. Locations of five whole round core samples used in these analyses. Note that seven were collected but two were deemed unsuitable for analysis.

Seabed Sampling

Core targets are shown in Figure 2. In general, areas that had minimal Holocene cover were selected. This was so the underlying glaciomarine mud could be sampled with the 2 m gravity corer, and often areas with no Holocene cover were covered by a lag surface and were challenging to core. Core 112gc was collected in a fiord, up-ice from a moraine, at the edge of a transition between current-swept lag surface and a "mud-mound". Cores 125gc and 127gc were collected in front of a moraine, itself down-ice stream of a hypothesised seabed volcano, similar in morphology to Kitasu Hill (Bednarski and Hamilton 2019). Note that the profile below has two turns in the middle, so that the left and right of the image are mirrored, but displaced to the NW. Core 127gc may have been collected in a mass transport deposit, however the base of which (where the geotechnical sample was extracted) was in glaciomarine sediments. Core 195gc was collected similarly proximal to a moraine in glaciomarine sediments, largely exposed (or remained without Holocene deposition) due to currents. Finally, core 197gc is collected in exposed seabed glaciomarine sediments. The absence of Holocene sediments likely due to currents steered along the adjacent bedrock.

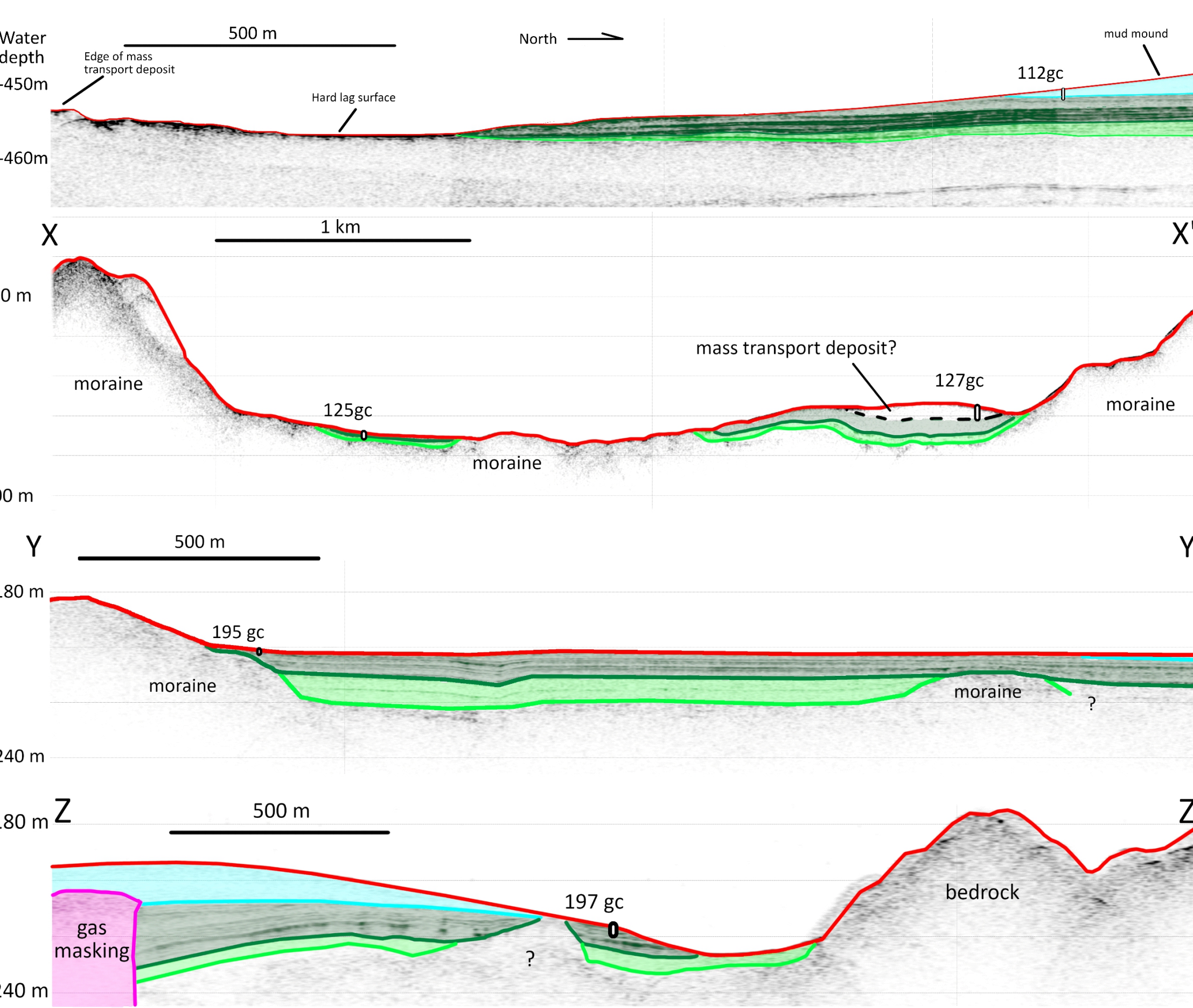


Figure 2 (above). 3.5 kHz subbottom profiles collected from 202106PGC showing the seismostratigraphy of each core location. Profile line locations shown in Figures 3 (X-X') and 4 (Y-Y' and Z-Z').

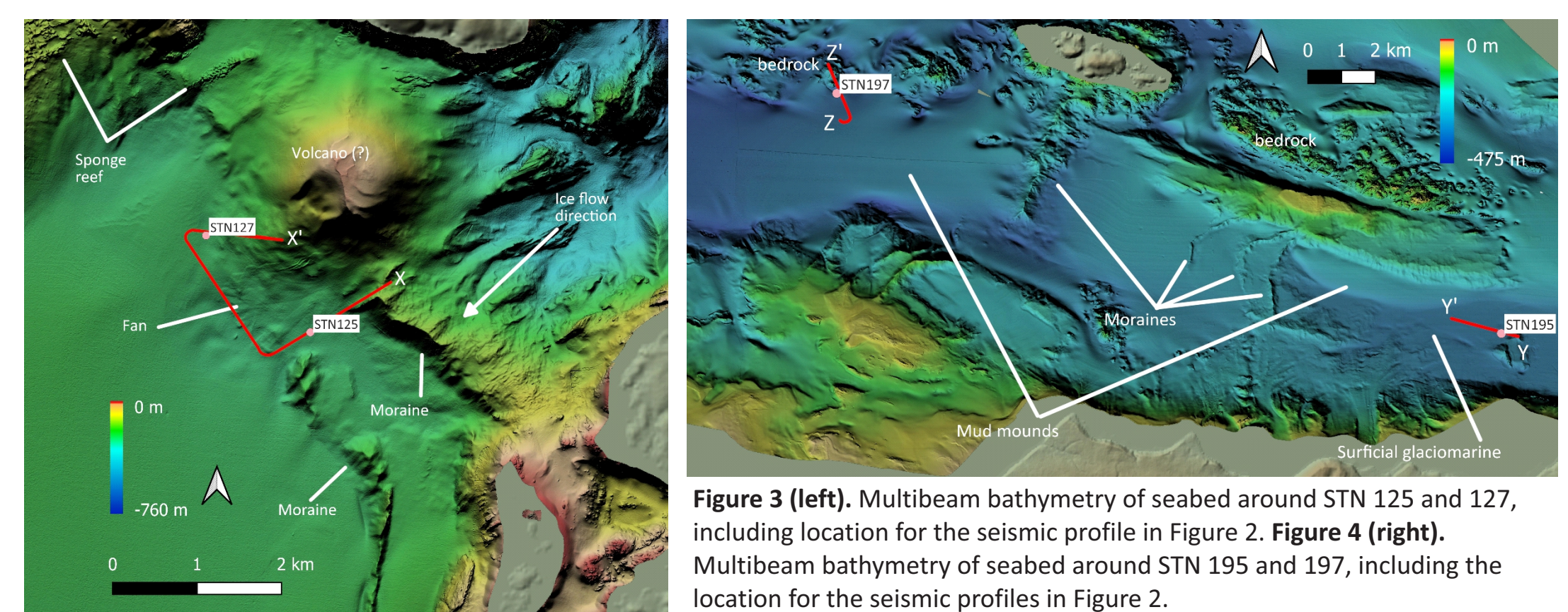


Figure 3 (left). Multibeam bathymetry of seabed around STN 125 and 127, including location for the seismic profile in Figure 2. Figure 4 (right). Multibeam bathymetry of seabed around STN 195 and 197, including the location for the seismic profiles in Figure 2.

References

Bednarski JM and Hamilton TS. 2019. Kitasu Hill: a Late-Pleistocene volcano, Swindle Island, British Columbia. Geological Survey of Canada, Open File 8593, 59p. <https://doi.org/10.4095/321052>
Eamer JBR, Levisky Z, MacKillop K. 2022. Geotechnical parameters important for offshore wind energy in Atlantic Canada. Geological Survey of Canada, Open File 8873, 41p. <https://doi.org/10.4095/329688>
Gourvenec S and White D. 2010. Gulf of Guinea Deepwater Sediments: Geotechnical Properties, Design Issues and Installation Experiences. Frontiers in Offshore Geotechnics II, CRC Press, Boca Raton, 59-86.
Ladd C and Foott R. 1974. New Design Procedure for Stability of Soft Clays, Journal of the Geotechnical Engineering Division, ASCE, vol. 100, No. GT7, pp. 763-786.
Lunne T, Berre T, Strandvik S. 1997. Sample disturbance effects in soft low plastic Norwegian clay. In Proceedings of the Conference on Recent Developments in Soil and Pavement Mechanics, Rio de Janeiro, Brazil, 25-27 June 1997. A.A. Balkema, Rotterdam, 81-102.
Ouellette D, MacKillop K, Lintern G, Stacey C, Fraser P. ND. Overview of geotechnical program in Kitimat Arm, Northern BC. Geological Survey of Canada, Open File XXXX, 1p. Available on request.
Skempton AW. 1970. The consolidation of clays by gravitational compaction. Quarterly Journal of the Geological Society of London 125, 373-412.
Sorensen KK, Okkels N, Winter MG, Smith DM, Eldred PJ, Toll DG. 2015. Correlation between compression index and index parameters for high plasticity Palaeogene clays. Geotechnical Engineering for Infrastructure and Development, 3371 – 3376.

Laboratory Analysis

Shipboard bulk density measurements were taken at 1 cm intervals using a Geotek whole core Multi-Sensor Core Logger (MSCL). An advanced geotechnical testing program was carried out at GSC-Atlantic geotechnical laboratory. The program was designed to determine sediment classification, strength parameters, stress history and sediment stiffness. The testing included 1) Atterberg Limits, 2) one dimensional consolidation tests and 3) isotopically consolidated undrained (CIU) triaxial with bender element tests.

Soil classification

In cores 125gc and 127gc the sediments are classified as high plasticity silts (MH) while the sediments in cores 112gc, 195gc and 197gc classify as low plasticity clays or silts (CL, Figure 5). The natural water content (w_n , %) for the 5 samples range from 40.6% to 93.4% (Table 1). Cores 125gc and 127gc have similar water content very similar MSCL density profiles with a negligible increase in values from a depth of 15 cm. (Figure 6). A sharp increase in density values mark the contact between the Holocene and the underlying glaciomarine sediments (i.e. 130 cm in core 112gc, 16 cm in core 125gc and 35 cm in core 197gc). Core 112gc density values show a linear, low variability increase in density values to 90 cm related to the Holocene sediments. The increase in variability from 90 cm to 130 cm in core 112gc may represent late Holocene reworking of the glaciomarine sediments.

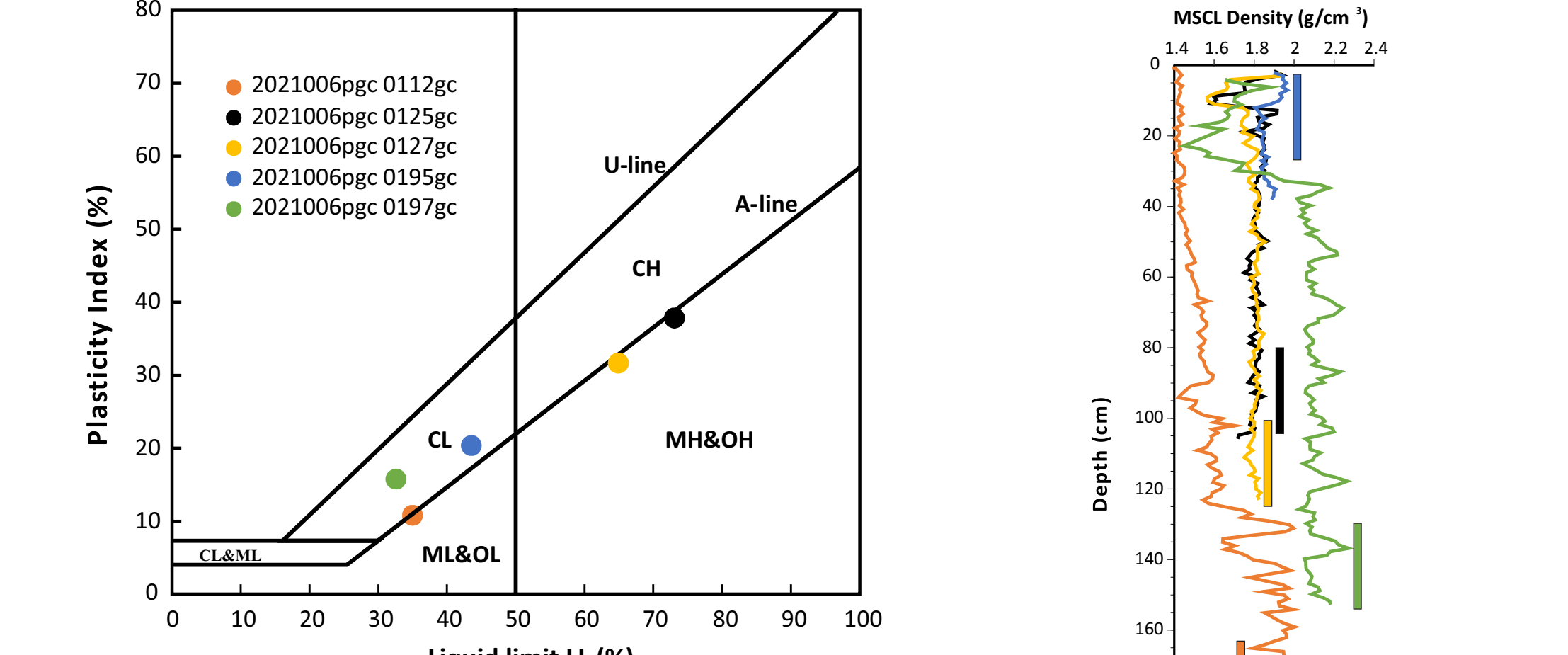


Figure 5. Plasticity chart showing the Atterberg limits results for 5 glaciomarine samples.

Core	Depth (cm)	w_n (%)	LL (%)	PL (%)	PI (%)	LI	Classification
202106PGC0112gc	174-188	56.2	35.0	24.2	10.8	3.0	CL
202106PGC0125gc	100-110	93.4	73.1	35.2	37.8	1.5	MH
202106PGC0127gc	121.5-130	84.9	64.9	33.3	31.7	1.6	MH
202106PGC0195gc	35-45	69.8	43.6	23.2	20.4	2.3	CL
202106PGC0197gc	152-158	40.6	32.6	16.9	15.8	1.5	CL

Consolidation Testing

Consolidation tests reproduce gravitational compaction (Skempton, 1970) in a controlled environment to simulate a sediment's response to vertical loading. The compressibility (C_c) and the rate of consolidation are used in seabed foundation design and depend on the sediment's composition, grain size distribution, hydraulic conductivity (k) and stress state described by the overconsolidation ratio (OCR). A sediment is normally consolidated if $OCR = 1$, overconsolidated if $OCR > 1$ and underconsolidated if $OCR < 1$. The C_c , k and OCR of the glaciomarine sediments were measured in 5 incremental loading consolidation tests with a load incremental ratio of 0.5. The preconsolidation stress (P'_c) was determined using Casagrande's method. The effective overburden stress (P'_v) was calculated by integrating the MSCL bulk density with depth. The samples are considered to be of fair quality (Lunne et al., 1997).

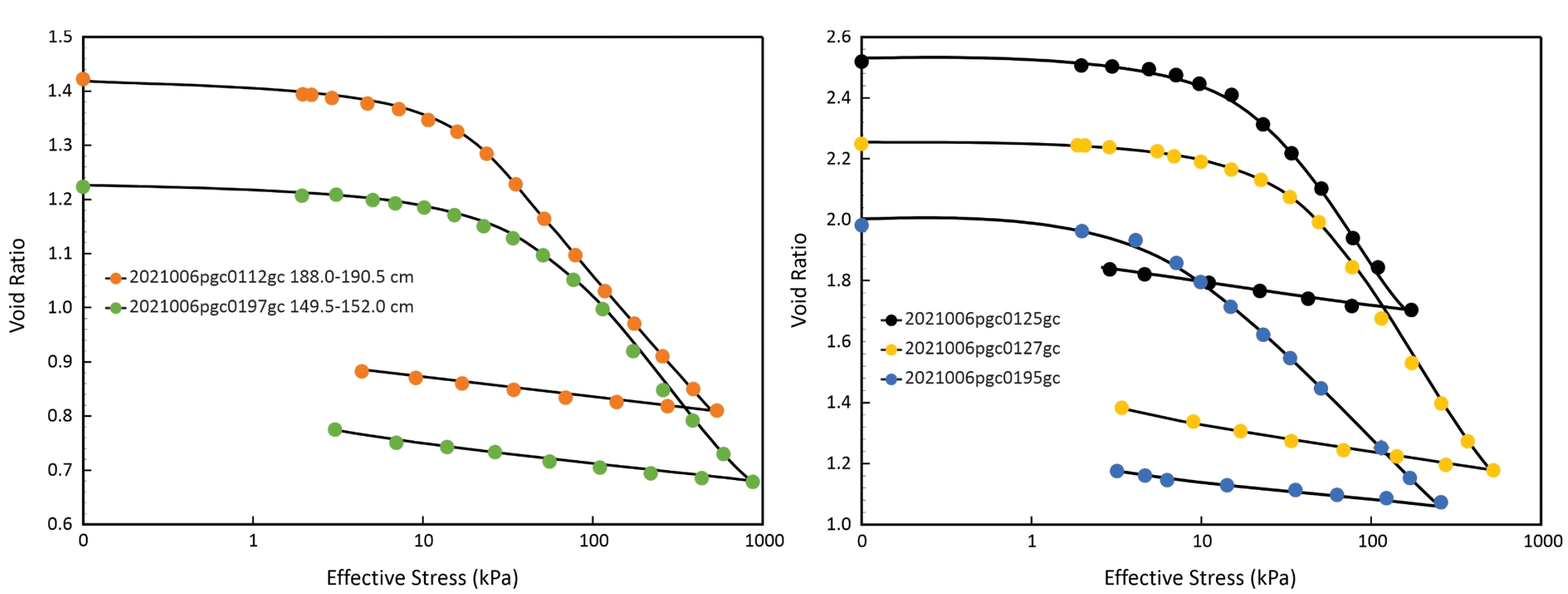


Figure 7. Consolidation plots for the 5 incremental loading consolidation tests of glaciomarine sediments

The sediments exhibit very similar consolidation curves (Figure 7). The sediments in 125gc and 127gc have high C_c (0.75 and 0.81) while sites 112gc and 197gc have intermediate C_c values (0.36 and 0.38). The recompression index (C_r) ranges from 0.034 to 0.085 and is approximately 10% of C_c . The sediments are over-consolidated showing a decrease in OCR with depth for cores 0195gc, 0125gc and 0112gc while OCR values are higher for cores 127gc and 195gc. The interpretation of stress history is difficult to interpret for marine sediments in the upper 2 m due to the effect of apparent overconsolidation (Gourvenec and White 2010). The sediment's k values at the estimated *in-situ* effective stress are typical for clayey silt. The consolidation test results are summarized in Table 2.

Core	Depth (cm)	P'_c (kPa)	P'_v (kPa)	OCR	C_c	C_r	k (m/s)	w_n (%)	e	G_s
202106PGC0112gc	188-190.5	18.0	11.23	1.60	0.36	0.034	1.36E-09	51.14	1.46	2.77
202106PGC0125gc	104-106.5	21.0	8.13	2.58	0.75	0.075	7.06E-09	93.43	2.52	2.69
202106PGC0127gc	122.5-125	37.5	9.39	3.99	0.81	0.085	2.46E-10	84.94	2.25	2.69
202106PGC0195gc	35.5-38	8.5	2.92	2.91	0.55	0.054	4.53E-09	72.11	1.47	2.76
202106PGC0197gc	149.5-152	52.0	14.60	3.56	0.38	0.036	1.94E-09	43.19	1.22	2.75

Acknowledgements

We thank the crew of the CCGS Vector for excellent support during data and sample collection in November of 2021. We also appreciate the logistical support from the Pacific Geoscience Centre (GSC-P) in packaging and shipping samples to GSC-A. Funding for this work was provided by Natural Resource Canada's Marine Geoscience for Marine Spatial Planning program. This poster benefitted from a careful and thorough peer-review by Kai Boggild, GSC-A.

Triaxial Testing

The shear strength of a sediment is the maximum resistance it displays against failure and is controlled by its effective stress. The strength characteristics of the marine sediments are paramount in evaluating seabed foundation conditions and submarine slope instability. The most common failure criteria applied to a sediment is the Mohr-Coulomb failure criterion, defined as $\tau_f = c' + \sigma'_v \tan \phi'$ where τ_f is the drained shear strength at failure, c' is the effective cohesion, σ'_v is the effective normal stress, and ϕ' is the effective internal angle of friction. The Mohr-Coulomb stress parameters (c' , ϕ') were determined from 5 isotopically consolidated undrained (CIU) triaxial tests. The normalized strength ratio S_u/σ'_v in the normal consolidation range was determined following Ladd and Foott's (1974) SHANSEP method.

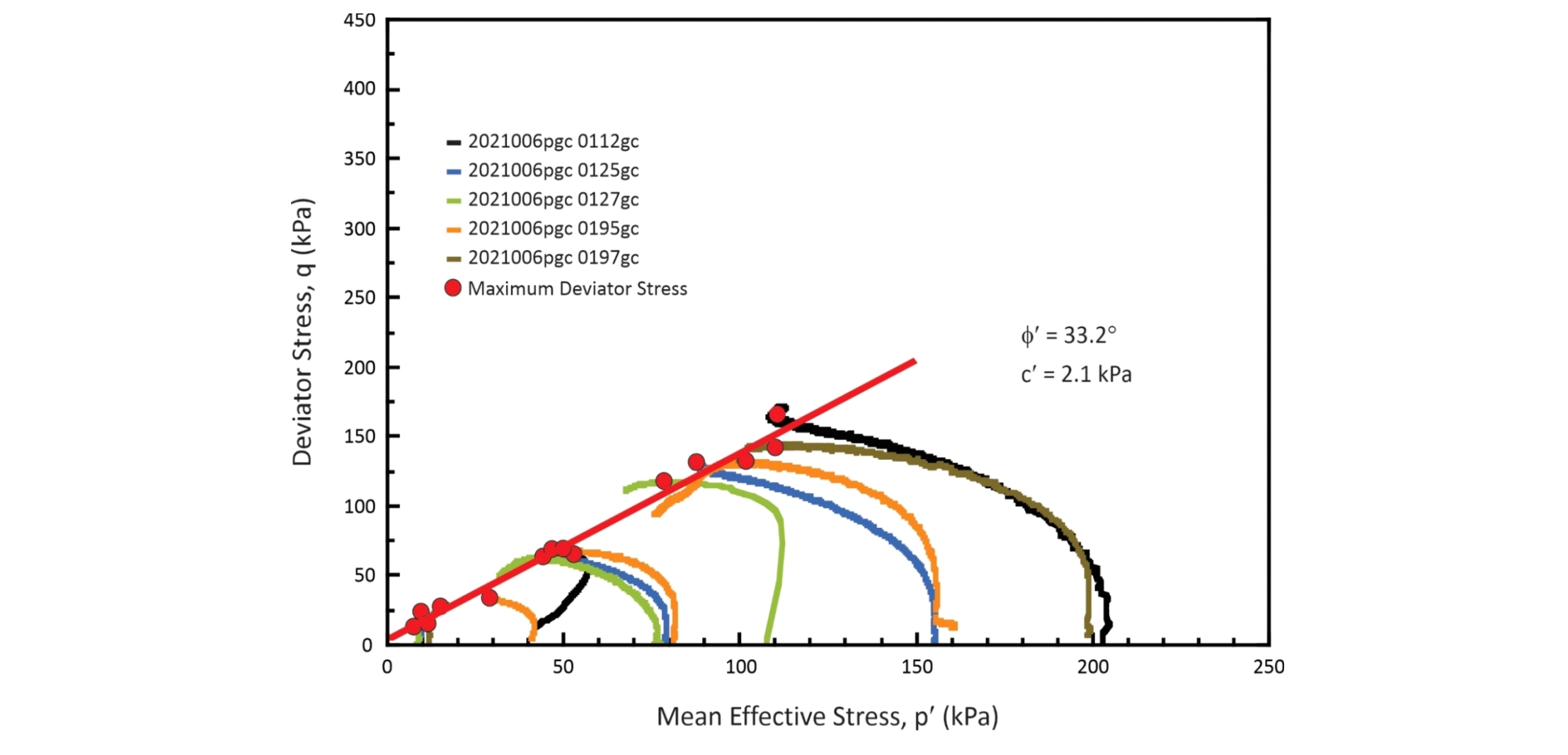


Figure 8. Stress paths and strength envelope for the glaciomarine sediments

The glaciomarine sediments from the 5 multi-stage CIU tests yield approximately the same failure envelopes (Figure 8). The points of maximum deviator stress plot into the failure envelope defined by $\phi' = 33.2^\circ$ and $c' = 2.1$ kPa. The S_u/σ'_v in the normal consolidation range varied from 0.29-0.36. Triaxial test results are summarized in Table 3.

Core	Depth (cm)	σ'_v (kPa)	c' (kPa)	A_1	w_n (%)	G_s	e	S_u/σ'_v	E_s (MPa)
202106PGC0112gc	175-187	32.1	2.20	0.46	56.21	2.77	1.54	0.29	5.66
202106PGC0125gc	91-103	35.9	1.76	0.26	83.68	2.69	2.12	0.34	3.99
202106PGC0127gc	109-121	34.5	3.10	0.22	82.18	2.69	2.38	0.36	3.90
202106PGC0195gc	5-17	32.4	0.00	NA	74.98	2.78	2.03	0.35	NA
202106PGC0197gc	137-149	31.1	3.62	0.15	43.80	2.76	1.18	0.30	5.51

Bender Element Testing

The bender element system enables the measurement of maximum shear modulus (G_{max}) of a soil at small strains in a triaxial cell. The shear modulus is used to characterize the sediment's stiffness and is related to a sediment's shear strength. The evaluation of G_{max} under static and dynamic loads is an important design criteria for the installations of wind turbines. G_{max} under static loading was calculated using $G_{max} = \sigma'_v \tan \phi' + S_{uv}$ where σ'_v is the bulk density and S_{uv} is the shear wave velocity, both measured at the end of each consolidation stage for the CIU tests.

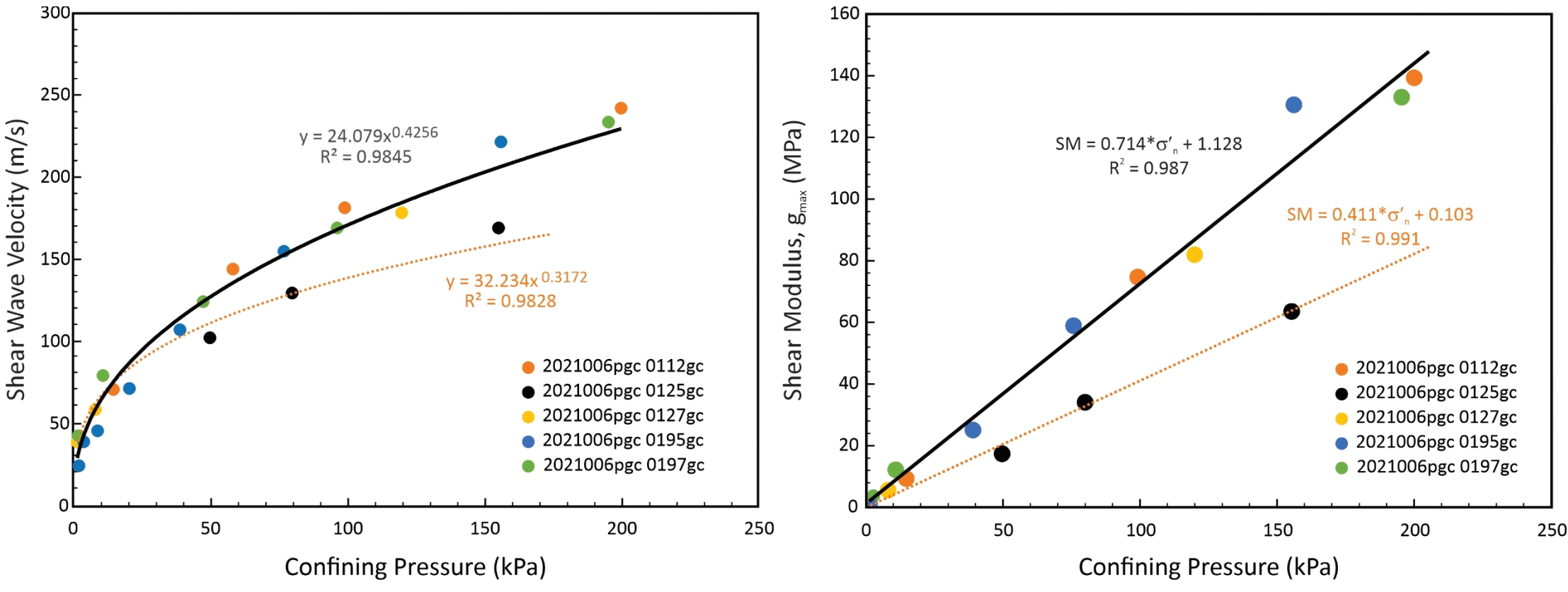


Figure 9. Shear wave velocity and shear modulus relationships with confining pressure.

For cores 112gc, 127gc, 195gc and 197gc there is a similar correlation between confining pressure and the shear wave velocity and the G_{max} for the glaciomarine sediments (Figure 9, solid line). For core 125gc there also good correlations with confining pressure however it is distinct from the other sites and requires further investigation to understand this difference (Figure 9, dashed line).

Findings

Cores 125gc and 127gc, located at the confluence of a glacial stillstand and a potential submarine volcano, showed unique characteristics when compared with other samples, including a higher plasticity (MH) and higher compressibility (C_c)—two indices that are correlated (Sorensen et al., 2015)—a higher natural and constant water content (w_n), and void ratio (e). The late-glacial paleoenvironment included a hypothesised eruption while ice was present (see example from nearby volcano in Bednarski and Hamilton (2019)); this may have resulted in a different depositional history and mineralogy (suggested by the lower specific gravity (G_s) and thus lower density/coarser materials). These two samples are the only two that occurred with a paired core indicating bioturbation at this depth, as well. Interestingly, cores 127gc and 195gc, uncorrelated geographically, are more overconsolidated than expected. This may be due to these two cores being most proximal to glacial moraine; resulted in high sedimentation near the ice front that has subsequently been eroded by strong currents. The higher OCR value for core 127gc may result if a mass transport deposit was sampled. Core 195gc may also be one of the oldest samples, likely from ice-proximal sedimentation. Core 125gc shows a unique shear modulus relationship with effective stress, suggesting a less stiff soil at this location. This could be attributed to the unique depositional environment found near the hypothesised volcano—in particular, 125gc is located in a small basin between two glacial moraines. However, the high similarity in the geotechnical parameters between cores 125gc and 127gc suggests that the difference in shear modulus may result from erroneous test data or sampling disturbance. The geotechnical test data of pre-Holocene glaciomarine sediments from similar regional geomorphologies (inner shelf fjord-type inlets) have different plasticity, compressibility and stress history but similar Mohr-Coulomb and small shear modulus parameters. A contributing factor to the different properties may be attributed to the occurrence of a volcanic eruption while ice was present.